Chemistry & Biology 13, 1217–1226, November 2006 DOI 10.1016/j.chembiol.2006.09.013

A Fluorescent Broad-Spectrum Proteasome Inhibitor for Labeling Proteasomes In Vitro and In Vivo

Martijn Verdoes,[1,5] Bogdan I. Florea,[1,5] Victoria Menendez-Benito,[2] Christa J. Maynard,[2] Martin D. Witte,[1] Wouter A. van der Linden,[1] Adrianus M.C.H. van den Nieuwendijk,[1] Tanja Hofmann,[1] Celia R. Berkers,[3] Fijs W.B. van Leeuwen,[3] Tom A. Groothuis,[4] Michiel A. Leeuwenburgh,[1] Huib Ovaa,[3] Jacques J. Neefjes,[4] Dmitri V. Filippov,[1] Gijs A. van der Marel,[1] Nico P. Dantuma,[2] and Herman S. Overkleeft[1,*]

[1] Bio-organic Synthesis
Leiden Institute of Chemistry
Leiden University
2300 RA Leiden
The Netherlands

[2] Department of Cell and Molecular Biology
The Medical Nobel Institute
Karolinska Institutet
SE-171 77 Stockholm
Sweden

[3] Division of Cellular Biochemistry

[4] Division of Tumor Biology
Netherlands Cancer Institute
1066 CX Amsterdam
The Netherlands

Summary

The proteasome is an essential evolutionary conserved protease involved in many regulatory systems. Here, we describe the synthesis and characterization of the activity-based, fluorescent, and cell-permeable inhibitor Bodipy TMR-Ahx$_3$L$_3$VS (MV151), which specifically targets all active subunits of the proteasome and immunoproteasome in living cells, allowing for rapid and sensitive in-gel detection. The inhibition profile of a panel of commonly used proteasome inhibitors could be readily determined by MV151 labeling. Administration of MV151 to mice allowed for in vivo labeling of proteasomes, which correlated with inhibition of proteasomal degradation in the affected tissues. This probe can be used for many applications ranging from clinical profiling of proteasome activity, to biochemical analysis of subunit specificity of inhibitors, and to cell biological analysis of the proteasome function and dynamics in living cells.

Introduction

The 26S proteasome is the central protease in ATP- and ubiquitin-dependent degradation of proteins in the eukaryotic cytoplasm and nucleus and is responsible for the degradation of 80%–90% of all cellular proteins. The proteasome is involved in the degradation of abnormal and damaged proteins, cell-cycle regulators, oncogens, and tumor suppressors, and it is imperative in the generation of MHC class I antigenic peptides [1]. Eukaryotic proteasomes contain two copies of seven distinct α and β subunits each. These subunits assemble into two types of heterooligomeric rings that are each composed of seven subunits (α1–α7 and β1–β7). The 20S proteasome is formed by two juxtaposed rings of β subunits flanked on top and bottom by a ring of α subunits [2]. When capped by the 19S regulatory complex at both ends, the proteolytically active 26S proteasome is formed and is responsible for ATP-dependent proteolysis of polyubiquitinated target proteins [3].

In the eukaryotic proteasome, three of the seven β subunits are responsible for the proteolytic activities of the proteasome. Characterization of the active β1, β2, and β5 subunits led to the classification of their substrate specificity as peptidylglutamyl peptide hydrolytic, trypsin-like, and chymotrypsin-like, respectively. In immune-competent cells, three additional active β subunits (βi) are expressed upon interferon-γ stimulation. These subunits assemble in a new proteasome particle called the immunoproteasome, which coexists with the constitutive proteasome [2].

The proteolytic subunits β1, β2, and β5 and their immunoproteasomal counterparts, β1i, β2i, and β5i, respectively, act by nucleophilic attack of the γ-hydroxyl of the N-terminal threonine on the carbonyl of the peptide bond destined for cleavage. The α-amine of the threonine acts as a base in the catalytic cycle. The existence and evolutionary development of six different active β subunits, their divergent substrate specificities, and their individual roles in cellular processes constitute a vast research field of interest in both academia and the pharmaceutical industry. This scientific demand can benefit from an activity-based proteasome probe that ideally (1) specifically targets the proteasome, (2) covalently and irreversibly binds to the three active β and βi subunits indiscriminately, (3) facilitates direct, rapid, accurate, and sensitive detection, (4) is cell permeable, and (5) enables monitoring of the proteasome by microscopic techniques in living cells.

To date, none of the available activity-based proteasome probes meet all of these requirements [4, 5]. The compound that comes closest is the radiolabeled proteasome inhibitor AdaY(^{125}I)Ahx$_3$L$_3$VS [6]. In this compound, the leucine vinyl sulfone mimics the peptide carbonyl and acts as a nucleophilic trap that covalently modifies the γ-hydroxyl of the N-terminal threonine through a Michael addition. This inhibitor is selective for the proteasome, labels the β subunits with equal intensity, and enables accurate and sensitive in-gel detection. However, usage of this activity-based probe is restricted to in vitro applications since this compound is not cell permeable. Recently, the weakly fluorescent and cell-permeable proteasome inhibitor dansyl-Ahx$_3$L$_3$VS was developed for profiling proteasome activity in living cells, enabling readout by antidansyl immunoblotting [7]. The low quantum yield and near-UV excitation of the dansyl makes this compound

*Correspondence: h.s.overkleeft@chem.leidenuniv.nl
[5] These authors contributed equally to this work.

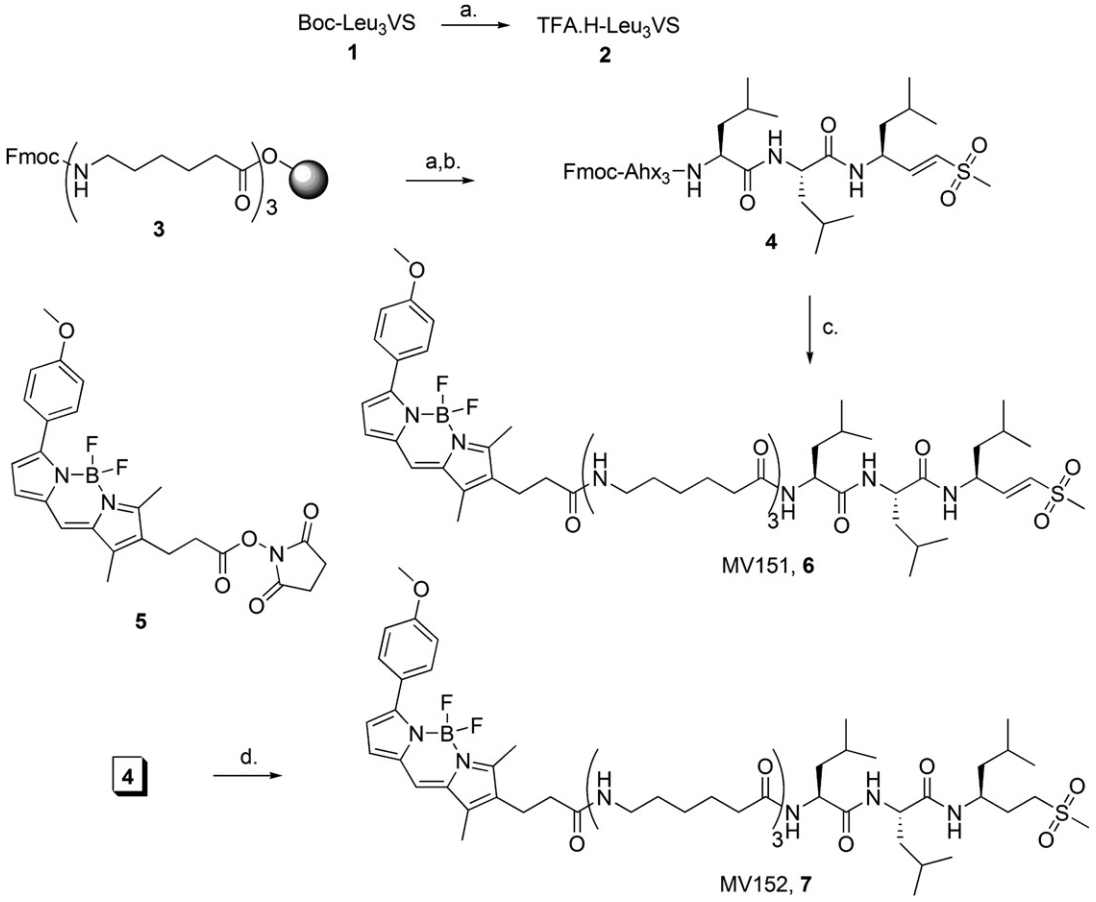

Figure 1. The Synthesis of Bodipy TMR-Ahx$_3$L$_3$VS, **6**, and the Control Compound Bodipy TMR-Ahx$_3$L$_3$ES, **7**

Reagents and conditions: (a) TFA/DCM 1/1 (v/v), 30 min. (b) **2** (2 equiv.), BOP (2.5 equiv.), DiPEA (6 equiv.), 12 hr, 98%. (c) (i) DBU (1 equiv.), DMF, 5 min; (ii) HOBt (4.5 equiv.), 1 min; (iii) **5** (1 equiv.), DiPEA (6 equiv.), 30 min, 99%. (d) (i) Pd/C, H_2, MeOH; (ii) DBU (1 equiv.), DMF, 5 min; (iii) HOBt (4.5 equiv.), 1 min; (iv) **5** (1 equiv.), DiPEA (6 equiv.), 30 min, 89%.

unsatisfactory for in-gel detection and standard fluorescence microscopic techniques.

Here, we present the synthesis and characterization of the fluorescent, cell-permeable, and activity-based proteasome probe Bodipy TMR-Ahx$_3$L$_3$VS (MV151). After proteasome labeling and protein separation by SDS-PAGE, the modified proteasome subunits are immediately visualized by in-gel fluorescence readout. Furthermore, this compound enables fast and sensitive labeling of proteasomes in vitro, in cells, and in mice; is compatible with live-cell imaging techniques; and facilitates screening and determination of the subunit specificity of novel proteasome inhibitors.

Results and Discussion

Synthesis of Bodipy TMR-Ahx$_3$L$_3$VS

Bodipy TMR-Ahx$_3$L$_3$VS (MV151, **6**) and the inactive, negative control, Bodipy TMR-Ahx$_3$L$_3$ES (MV152, **7**), in which the vinyl sulfone moiety is reduced to an ethyl sulfone, were synthesized as depicted in Figure 1. Acidic cleavage of Fmoc-Ahx$_3$-Wang resin (**3**), synthesized by using standard Fmoc-based solid-phase peptide chemistry, gave the crude Fmoc-Ahx$_3$-OH, which was block coupled to TFA·H-Leu$_3$VS (**2**) [8], to yield Fmoc-protected hexapeptide (**4**). In situ deprotection of the Fmoc-protecting group with DBU and treatment with Bodipy TMR succinimidyl ester (**5**) ([9–11, 12]; see the Supplemental Data available with this article online) afforded target compound **6**. In order to obtain the inactive control compound **7**, hexapeptide **4** was first treated with hydrogen gas and palladium on charcoal in methanol to reduce the vinyl sulfone, followed by Fmoc cleavage and introduction of the Bodipy TMR moiety.

Proteasome Labeling and In-Gel Detection

The potency of MV151 (**6**) was determined by measuring proteasomal activity by using fluorogenic substrates. EL-4 lysates were incubated with increasing concentrations of MV151, and the cleavage of the substrates Suc-Leu-Leu-Val-Tyr-AMC (chymotrypsin-like activity), Z-Ala-Ala-Arg-AMC (trypsin-like activity), and Z-Leu-Leu-Glu-βNA (peptidylglutamyl peptide hydrolytic activity) was monitored. At concentrations below 1 μM, MV151 appears to inhibit trypsin-like activity and chymotrypsin-like activity more efficiently than it inhibits PGPH activity (Figure 2A). This might be due to differences in activity between the subunits, to allosteric effects, to minor subunit specificities of the probe, or to nonsaturation kinetics. At concentrations of 1 μM and higher, MV151 completely inhibits all three activities.

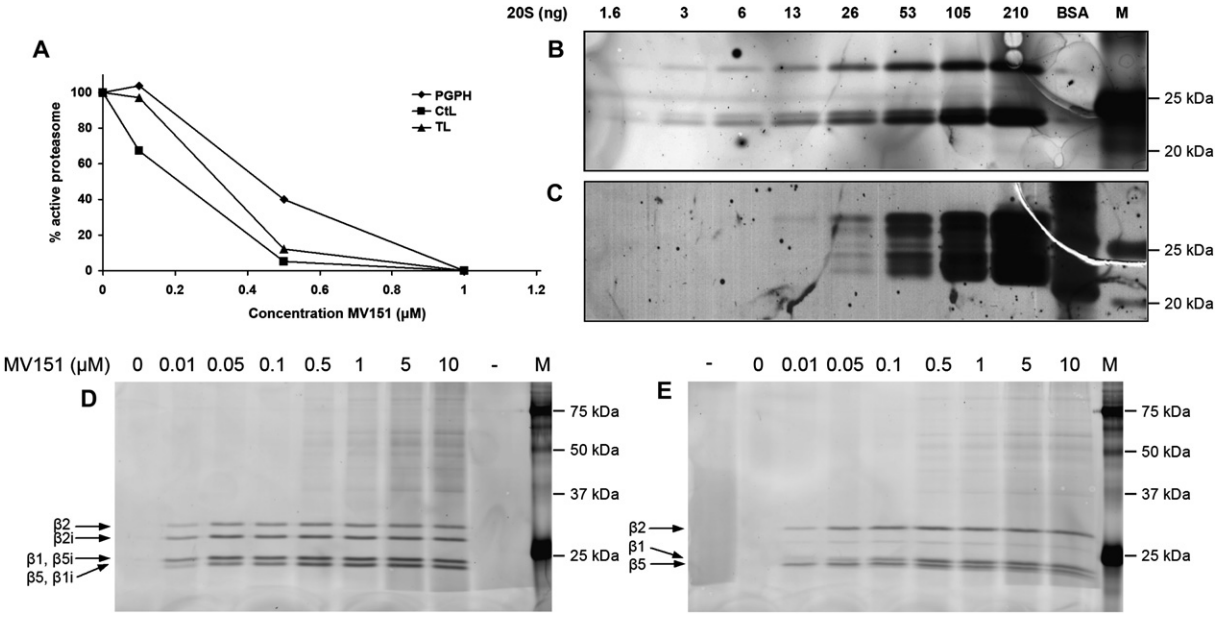

Figure 2. Proteasome Labeling and In-Gel Detection from Cell Extracts

(A) Measurement of proteasome activity with fluorogenic substrates after treatment of EL-4 lysates with the indicated concentrations of MV151 (PGPH, peptidylglutamyl peptide hydrolytic activity; TL, trypsin-like activity; CtL, chymotrypsin-like activity).

(B and C) Comparison between fluorescent in-gel detection and silver staining. The indicated amounts of purified human 20S proteasome and BSA (1 μg) were incubated for 1 hr at 37°C with 300 nM MV151, resolved by SDS-PAGE, and detected by (B) direct fluorescence in-gel readout and by (C) silver staining.

(D and E) Proteasome labeling profile in (D) EL-4 and (E) HeLa lysates (10 μg) incubated for 1 hr at 37°C with the indicated concentrations of MV151. "M" represents the molecular marker (Dual Color, BioRad); "−" represents heat-inactivated lysates incubated with 10 μM MV151 for 1 hr at 37°C.

Direct in-gel visualization of MV151-labeled proteasome subunits was explored by using a fluorescence scanner. Treatment of purified human 20S proteasome with MV151 showed uniform labeling of the active subunits β1, β2, and β5 (Figure 2B). To determine the sensitivity of the in-gel detection, we directly compared fluorescence readout of the gel (Figure 2B) with detection of proteasome subunits by silver staining of proteins (Figure 2C). The in-gel detection was shown to be very sensitive since as little as 3 ng proteasome was sufficient to detect individual MV151-labeled proteasome subunits; detection with this method is at least three times more sensitive than silver staining.

We next compared the labeling of the constitutive β1, β2, and β5 subunits and the immunoproteasome β1i, β2i, and β5i subunits. For this purpose, we labeled the proteasomes in lysates of the human cervix carcinoma cell line HeLa (expressing constitutive proteasome) and the murine lymphoid cell line EL-4 (expressing both constitutive and immunoproteasome) with increasing concentrations of MV151. All active constitutive and inducible β proteasome subunits were neatly and uniformly labeled by MV151 (Figures 2D and 2E). All subunits were already detectable at a concentration of 10 nM MV151 and reached saturation in fluorescence signal at 1 μM MV151. At higher concentrations of MV151, an increased nonspecific labeling was observed in the high molecular weight region.

Proteasome Profiling Screen of Known Inhibitors

Next, we performed competition experiments with MV151 to determine the subunit specificity of a panel of known proteasome inhibitors. EL-4 and HeLa cell lysates (10 μg total protein) were first incubated for 1 hr with the inhibitor of interest. After incubation with the proteasome inhibitor, the subunits that were still active were fluorescently labeled by treating the lysates with 100 nM MV151 for 1 hr.

In HeLa lysates, epoxomicin preferentially inhibits the β5 subunit, already visible at a 10 nM concentration. At epoxomicin concentrations over 100 nM, β1 and β2 are also targeted, with a slight preference for β2 (at 5 μM epoxomicin, β2 fluorescence is absent and a faint band of β1 is still visible) (Figure 3A, right panel). This is in accordance with the inhibition profile of epoxomicin determined with purified 20S proteasome [12]. Interestingly, in EL-4 lysates, epoxomicin preferentially inactivates β2 and β2i and is less active toward constitutive and immunoinduced β1 and β5 subunits (Figure 3A, left panel).

Dansyl-Ahx$_3$L$_3$VS [7] inhibits all active constitutive and immunoinduced subunits in EL-4 from concentrations of 500 nM and greater (Figure 3B, left panel). In HeLa lysates, dansyl-Ahx$_3$L$_3$VS has a preference for the β5 subunit, which is visible at 100 nM, and less of a preference for the β1 and β2 subunits, which are visible at slightly higher concentrations (Figure 3B, right panel).

The dipeptidyl pinanediol boronic ester (pinanediol boronic ester of Bortezomib [13]) shows a strong selectivity for the constitutive β1 and β5 subunits in HeLa lysates (Figure 3C, right panel) and β1, β1i, β5, and β5i in EL-4 lysates (Figure 3C, left panel). The inhibition profile of the dipeptidyl pinanediol boronic ester is comparable to the labeling profile of Bortezomib [7], with potency in the same order of magnitude.

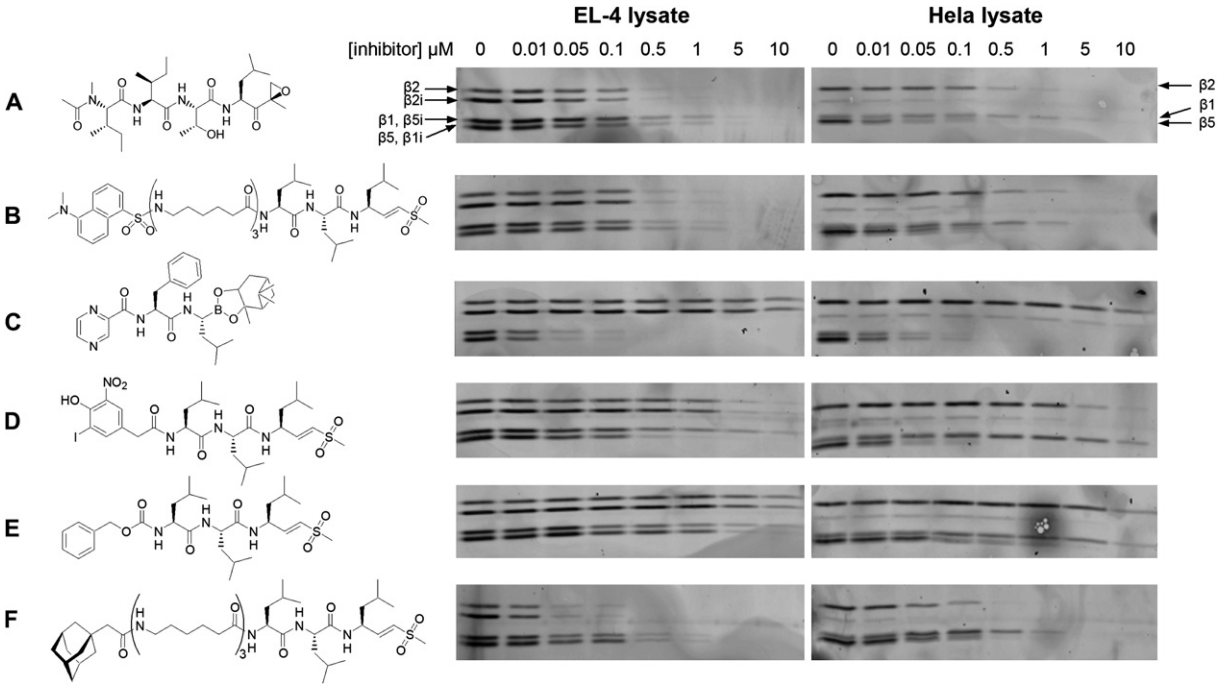

Figure 3. Proteasome Profiling Screen of Known Inhibitors by Using MV151

(A–F) EL-4 and HeLa lysates (10 μg total protein) were incubated with the indicated concentrations of the (A) proteasome inhibitor epoxomicin, (B) dansyl-Ahx$_3$L$_3$VS, (C) dipeptidyl pinanediol boronic ester, (D) NLVS, (E) ZLVS, and (F) Ada-Ahx$_3$L$_3$VS for 1 hr at 37°C. The remaining activity of the β subunits was fluorescently labeled by incubation with 0.1 μM MV151 for 1 hr at 37°C.

As previously reported, NLVS [8] shows a predilection for β5 (Figure 3D), whereas ZLVS [8] (Figure 3E) proves to be the least potent compound and shows some preference for constitutive and immunoinduced β1 and β5 subunits.

In EL-4 lysates, ada-Ahx$_3$L$_3$VS [6] first targets the β2 and β2i subunits, and it shows a preference for β2 and β5 in HeLa lysates (Figure 3F).

Altogether, this experiment shows that MV151 can be used for the determination of inhibition profiles of proteasome inhibitors. Exploiting the sensitivity of in-gel detection of MV151, it is possible to demonstrate that the inhibitors tested show subtle differences in the proteasome inhibition profile.

Functional Proteasome Inhibition in Living Cells

We next addressed whether MV151 is able to label proteasome subunits in living cells. EL-4 and HeLa cells were incubated with increasing concentrations of MV151. Specific and sensitive labeling of all proteasome subunits was observed in EL-4 (Figure 4A) and HeLa cells (Figure 4B), although higher concentrations were required than for labeling of subunits in lysates. Labeling of the β1 subunit shows a lower intensity than in lysates, whereas β5 labeling looks more pronounced. This difference in the labeling profile between the proteasome in cell lysates and living cells has been previously reported [7]; however, the reason for this remains unclear. Importantly, incubation of EL-4 and HeLa cells with the inactive control compound MV152 (7), which is almost identical to MV151 but lacks the reactive vinyl sulfone warhead, showed no labeling of the proteasome or any other protein (Figures 4A and 4B).

In vivo functionality of MV151 was determined in HeLa cells stably expressing a green fluorescent protein (GFP) reporter proteasome substrate [14]. The ubiquitin^{G76V}-GFP (Ub^{G76V}-GFP) fusion expressed by these cells is normally rapidly degraded by the proteasome. Indeed, untreated Ub^{G76V}-GFP HeLa cells emitted only low levels of GFP fluorescence (Figure 4C, left panel). Cells that were exposed to 10 μM of the inactive MV152 for 12 hr did accumulate the control compound, but they did not show increased levels of GFP fluorescence (Figure 4C, middle panel). During 12 hr of exposure to 10 μM MV151, cells accumulated the inhibitor and showed significantly increased levels of GFP fluorescence (Figure 4C, right panel). Strong fluorescence is apparent in the membranous compartments of cells treated with the inactive MV152. This fluorescence, which appears to be stronger than in MV151-treated cells, and which is not due to proteasome labeling (as judged from SDS-PAGE analysis), is likely due to accumulation of MV152 in the hydrophobic environment of the membranes. The active MV151 is likely not to accumulate in the lipid bilayers, because it is sequestered by the proteasome active sites. It should be noted that Bodipy dyes fluoresce strongly in hydrophobic environments. There was no visual evidence of cellular toxicity at the dose and exposure time used in this study. These results were confirmed by a study with the human melanoma cell line MelJuSo stably expressing the N-end-rule reporter proteasome substrate Ub-R-GFP [14] (data not shown).

We next set out to determine whether the intracellular staining pattern of MV151 colocalized with the proteasome in living cells. To this end, we used MelJuSo cells

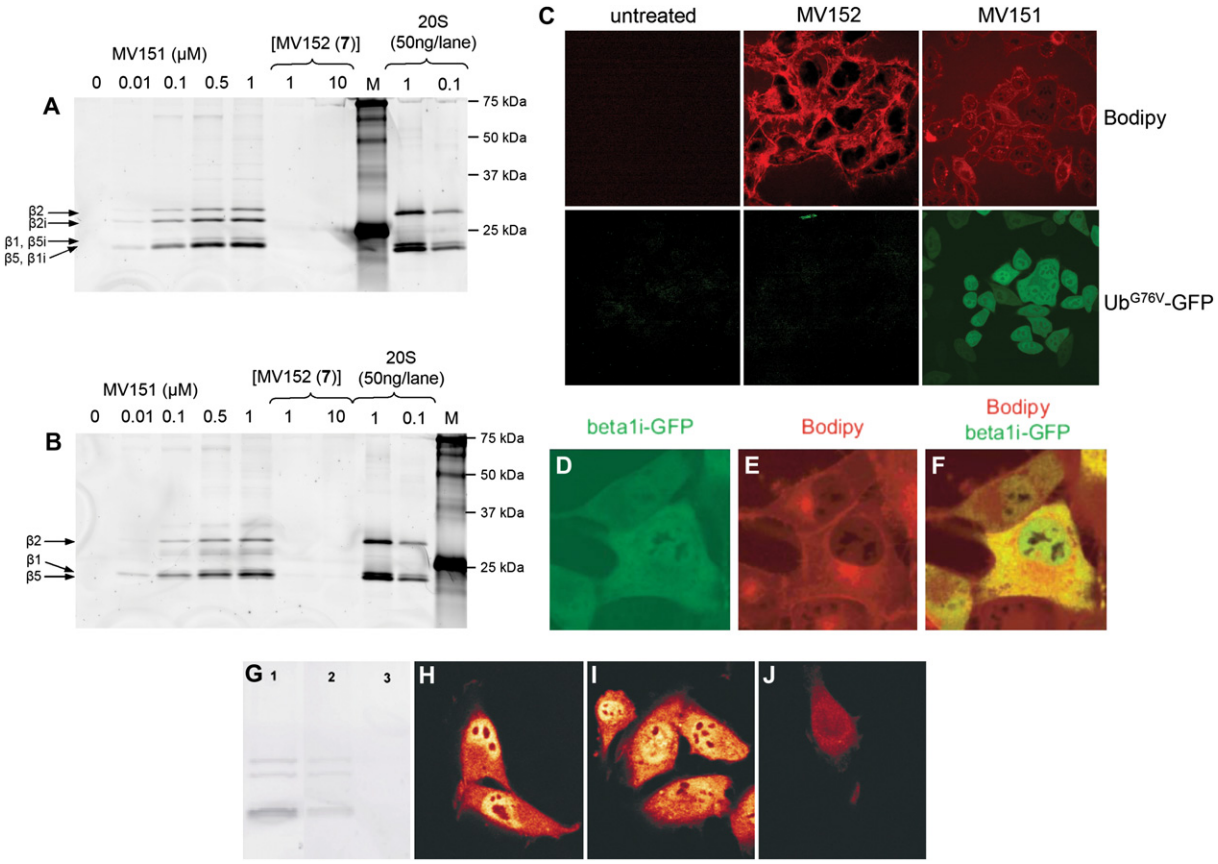

Figure 4. Functional Proteasome Inhibition in Living Cells

(A and B) Proteasome profiling in living (A) EL-4 and (B) HeLa cells after a 2 hr incubation with the indicated concentrations of MV151. As a control, the cells were incubated with the inactive compound MV152. A purified proteasome labeled with MV151 is also shown.

(C) Representative micrographs of Ub^{G76V}-GFP HeLa cells that were untreated (left panel), incubated for 12 hr with 10 μM inactive MV152 (middle panel), and incubated for 12 hr with 10 μM MV151 (right panel). Bodipy TMR and Ub^{G76V}-GFP fluorescence are shown.

(D–F) Colocalization of a GFP-labeled proteasome and MV151 in living GFP-β1i MelJuSo cells treated for 8 hr with 10 μM MV151. (D) GFP- β1i, (E) Bodipy TMR fluorescence, and (F) a merged image are shown.

(G) In-gel visualization of proteasome labeling in living EL-4 cells: lane 1, a 1 hr incubation with MV151 (250 nM); lane 2, a 1 hr incubation with MV151 (250 nM), followed by a 1 hr incubation with MG132 (5 μM); lane 3, a 1 hr incubation with MG132 (5 μM), followed by a 1 hr incubation with MV151 (250 nM).

(H–J) CLSM pictures of Bodipy TMR fluorescence in MelJuSo Ub-R-GFP cells after formaldehyde fixation, gain 700. (H) Confocal picture after a 1 hr incubation with MV151 (500 nM). (I) Confocal picture after a 1 hr incubation with MV151 (500 nM), followed by a 1 hr incubation with MG132 (5 μM). (J) Confocal picture after a 1 hr incubation with MG132 (5 μM), followed by a 1 hr incubation with MV151 (500 nM).

that stably express a GFP-tagged β1i proteasome subunit, which is efficiently incorporated into the proteasome particles [15]. The GFP-β1i fusion construct shows ubiquitous distribution throughout the cytoplasm and nucleus, with exception of nucleoli and the nuclear envelope (Figure 4D). The GFP-β1i cells were incubated with 10 μM MV151 and the distribution of proteasomes and inhibitor was compared. The intracellular permeation of MV151 was monitored in time and is characterized by a fast permeation phase (several minutes), followed by a slow distribution phase (several hours, data not shown). During the permeation phase, the compound showed significant association with the plasma membrane, in discrete cytoplasmatic vesicular and membranous fractions and at the nuclear envelope.

After 5 hr of distribution, MV151 is localized throughout the cell, with the exception of the nucleoli, similar to the GFP-β1i fusion (Figures 4D–4F). The fact that MV151 is excluded from the nucleoli is in line with the idea that the compound is associated with the proteasome. In some cells, granular accumulation of MV151 was observed in the cytoplasm in close proximity to the nucleus.

To attest whether the in-gel readout could be correlated with the fluorescent microscopy data, MV151 was competed with the proteasome inhibitor MG132 (Figures 4G–4J). MelJuSo Ub-R-GFP cells incubated with MV151 for 1 hr showed labeling of the active proteasome subunits on gel (Figure 4G, lane 1) and, after fixation with formaldehyde, strong fluorescence in the cytoplasm and nucleus, with the exception of nucleoli (Figure 4H). In Figure 4I, cells incubated with MV151 for 1 hr, followed by a 1 hr incubation with MG132, showed labeling of the active proteasome subunits on gel (Figure 4G, lane 2) and a similar cellular localization to that shown in Figure 4H. When the cells where first

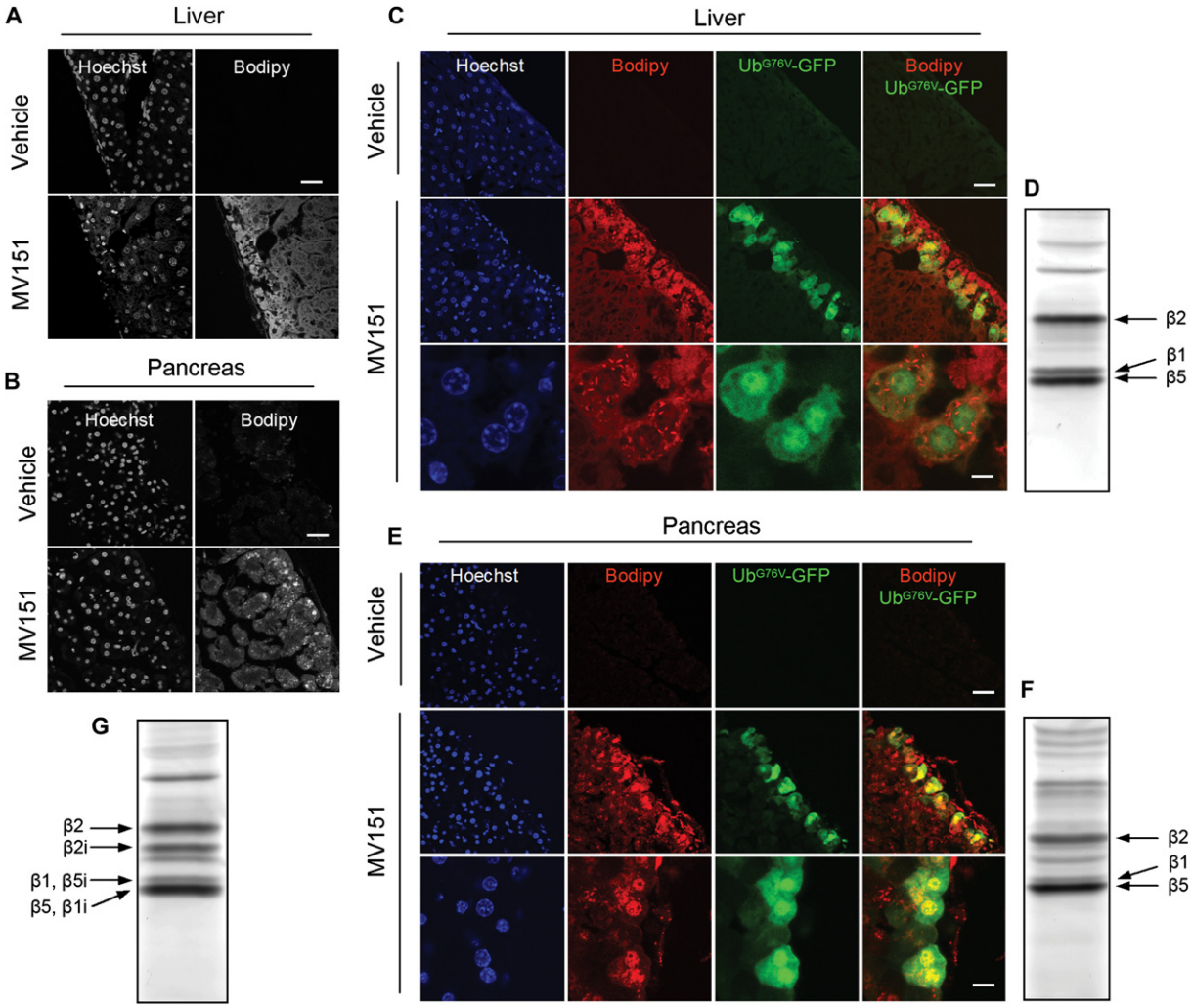

Figure 5. Functional Proteasome Inhibition in Mice

(A and B) Micrographs of (A) liver and (B) pancreas cryosections from C57Bl/6 mice that were treated with vehicle only or with MV151 (20 μmol/kg body weight). Hoechst staining and Bodipy TMR fluorescence are shown. The scale bar represents 40 μm.

(C–G) Micrographs and in-gel fluorescence readout of (C and D) liver and (E and F) pancreas. (C and E) Cryosections from Ub^{G76V}-GFP mice that were treated with vehicle only or with MV151 (20 μmol/kg body weight). Hoechst staining, Bodipy TMR fluorescence, Ub^{G76V}-GFP fluorescence, and Bodipy TMR and Ub^{G76V}-GFP merged images are shown. The scale bar represents 40 μm (upper and middle panels) and 5 μm (lower panels). (D and F) SDS-PAGE analysis and in-gel fluorescence readout of homogenates (10 μg total protein) from liver and pancreas tissues shown in (C) and (E), respectively, and (G) in spleen.

incubated with MG132 for 1 hr, followed by a 1 hr incubation with MV151, in-gel readout proved negative (Figure 4G, lane 3) and the fluorescence in the cells had dramatically decreased (Figure 4J). This competition study proves that the vast majority of the fluorescence observed in cells, after fixation, is due to proteasome labeling.

Monitoring of Proteasome Inhibition in Mice

The results obtained in cell lines prompted us to investigate whether MV151 could be used to label proteasomes in mice. To test the bioavailability of MV151, C57Bl/6 mice were given a single intraperitoneal injection with MV151 (20 μmol/kg body weight) and were sacrificed 24 hr postinjection.

Fluorescence microscopic analysis of mouse tissues revealed the capacity of MV151 to penetrate tissues in vivo. The highest Bodipy TMR fluorescence was detected in the liver (Figure 5A) and in the pancreas (Figure 5B). Interestingly, Bodipy TMR fluorescence was higher in the peripheries of the tissues, indicating that the probe might reach the liver most efficiently by diffusion from the peritoneal cavity rather than being distributed by entering the bloodstream.

To examine the effect of administration of the proteasome probe, we took advantage of a recently developed transgenic mouse model for monitoring the ubiquitin-proteasome system, which is based on the ubiquitous expression of the Ub^{G76V}-GFP reporter [16]. We have previously shown that administration of the proteasome inhibitors epoxomicin and MG262 results in a substantial accumulation of the Ub^{G76V}-GFP reporter in affected tissues [16]. The accumulation was primarily found in the liver and at higher concentrations in other tissues. In the present experiment, the Ub^{G76V}-GFP reporter mice were given a single intraperitoneal injection with

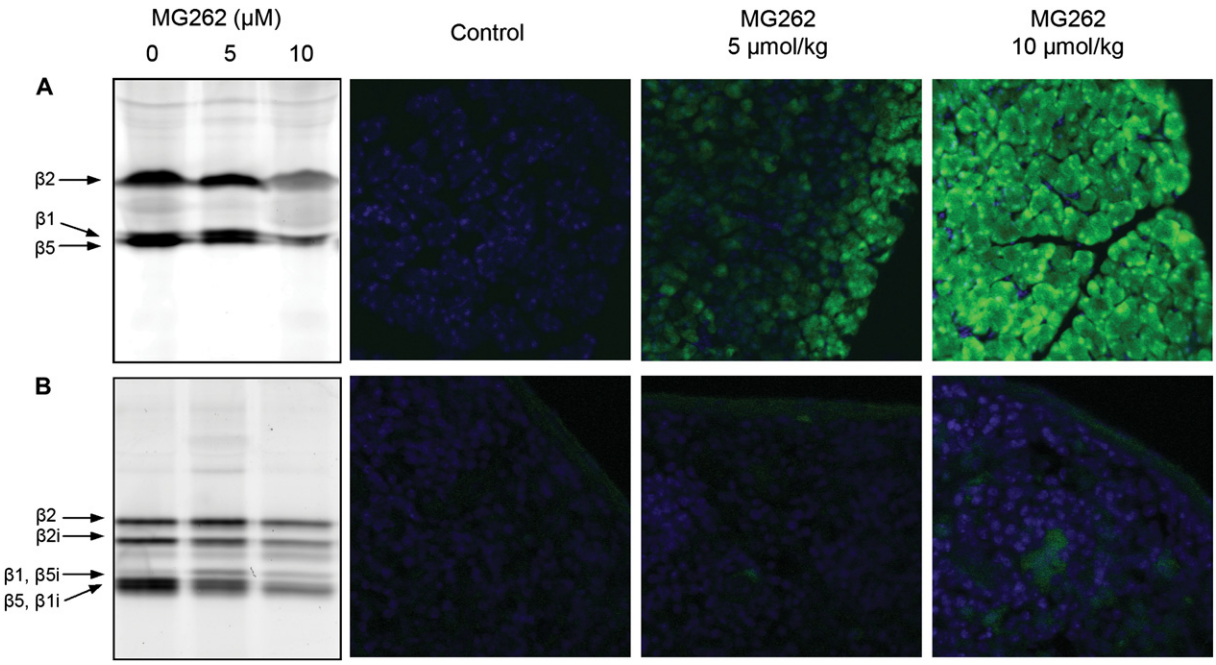

Figure 6. MG262 Biodistribution Study in Ub^{G76V}-GFP Reporter Mice, followed by MV151 In-Gel Fluorescence Readout

(A and B) Ub^{G76V}-GFP reporter mice were treated with 0, 5, or 10 μmol/kg bodyweight MG262 by intraperitoneal injection and were sacrificed after 24 hr. (A) Pancreas and (B) spleen were analyzed. Remaining activity of the β subunits in tissue homogenates was fluorescently labeled by incubation with 0.1 μM MV151 for 1 hr at 37°C. Cryosections of fixed (A) pancreas and (B) spleen were analyzed for accumulation of the reporter by confocal microscopy; green, GFP; blue, Hoechst nuclear stain.

MV151 (20 μmol/kg body weight). A total of 24 hr postinjection, the mice were sacrificed and several tissues were analyzed by fluorescence microscopy. Cells accumulating Ub^{G76V}-GFP were detected in the liver (Figure 5C) and the pancreas (Figure 5E), which also contained the highest Bodipy TMR fluorescence of all of the examined tissues (spleen, intestine, kidney, liver, and pancreas). Importantly, all of the cells that accumulated the Ub^{G76V}-GFP reporter contained very high Bodipy TMR fluorescence. The proteasome probe was distributed both in the cytoplasm and nuclei of the cells that accumulated the reporter. Similar to our observations from experiments in cell culture, the affected cells in the mice contained granular accumulations of MV151 in the cytoplasm in close proximity to the nucleus. We verified that accumulation of Ub^{G76V}-GFP in the liver and pancreas coincided with proteasomal blockade by MV151. SDS-PAGE followed by in-gel fluorescence analysis of liver (Figure 5D) and pancreas (Figure 5F) homogenates of animals treated with MV151 revealed that the proteasome catalytic subunits were labeled as expected, although higher background labeling compared to in vitro studies was observed. (For Figures 5D and 5F, respectively, the tissues from the images in Figures 5C and 5E were used.) SDS-PAGE followed by in-gel fluorescence analysis of spleen homogenates showed labeling of both constitutive and inducible proteasome catalytic subunits (Figure 5G).

As the final set of experiments, we monitored the biodistribution of MG262 in Ub^{G76V}-GFP transgenic mice. We selected the boronic acid MG262 for this purpose because it is both commercially available in purified form and most closely resembles the drug Bortezomib. Animals were injected subcutaneously with either 5 μmol/kg or 10 μmol/kg body weight of the boronic acid MG262 and were sacrificed 24 hr postinjection. Spleen and pancreas were lysed and treated with MV151. SDS-PAGE analysis revealed significant reduction of labeled bands corresponding to the proteasome catalytic subunits when compared with tissue lysates from untreated animals (Figure 6A, pancreas; Figure 6B, spleen). Fluorescence microscope analysis of the same tissues (Figures 6A and 6B) confirmed the concentration-dependent inhibition of the proteasome in MG262-treated Ub^{G76V}-GFP mice, as indicated by increased levels of Ub^{G76V}-GFP reporter accumulation.

In summary, we described the synthesis of MV151 and characterized it as being a cell-permeable, broad-spectrum proteasome inhibitor. MV151 enables broad-spectrum proteasome profiling, both in cell lysates and in living cells. The Bodipy TMR dye proved to be very useful for in-gel readout of labeled active subunits in that it provided a straightforward method for direct and sensitive proteasome profiling and omitted the need for western blotting, radioactivity, and gel drying. MV151 could be readily detected upon administration to mice and correlated with inhibition of the proteasome in the affected tissues. Finally, MV151-mediated proteasome labeling in combination with Ub^{G76V}-GFP transgenic mice is a useful strategy for monitoring the biodistribution of proteasome inhibitors.

Significance

The proteasome is a key enzyme in the maintenance of cellular homeostasis. Here, the synthesis and

characterization of the activity-based, fluorescent, and cell-permeable MV151 are presented. MV151 targets the proteasome specifically and shows broad-spectrum activity by covalent and irreversible binding to the catalytic N-terminal threonine residues of immunoinducible and constitutively active β subunits. The bright fluorophore facilitates rapid and sensitive detection of active proteasome subunits by in-gel detection and fluorescence microscopy in living cells. Potentially, MV151 can find application in diverse fields of proteasome research: in medical research, for profiling the active proteasome fractions in a clinically relevant sample; and in chemistry and biochemistry, facilitating rapid determination of potency and subunit specificity of new proteasome inhibitors.

Experimental Procedures

Synthesis

General Methods and Materials

All reagents were commercial grade and were used as received unless indicated otherwise. Toluene (Tol.) (purum), ethyl acetate (EtOAc) (puriss.), and light petroleum ether (PetEt) (puriss.) were obtained from Riedel-de Haën and were distilled prior to use. Dichloroethane (DCE), dichloromethane (DCM), dimethyl formamide (DMF), and dioxane (Biosolve) were stored on 4 Å molecular sieves. Tetrahydrofuran (THF) (Biosolve) was distilled from $LiAlH_4$ prior to use. Reactions were monitored by TLC analysis by using DC-fertigfolien (Schleicher & Schuell, F1500, LS254) with detection by UV absorption (254 nm), spraying with 20% H_2SO_4 in ethanol, followed by charring at ~150°C; by spraying with a solution of $(NH_4)_6Mo_7O_{24}C4H_2O$ (25 g/L) and $(NH_4)_4Ce(SO_4)_4C2H_2O$ (10 g/L) in 10% sulfuric acid, followed by charring at ~150°C; or by spraying with an aqueous solution of $KMnO_4$ (7%) and KOH (2%). Column chromatography was performed on Merck silicagel (0.040–0.063 nm). Electrospray ionization mass spectra (MS [ESI]) were recorded on a PE/Sciex API 165 instrument interface, and HRMS (SIM mode) were recorded on a TSQ Quantum (Thermo Finnigan) fitted with an accurate mass option, interpolating between PEG calibration peaks. ^{1}H- and ^{13}C-APT-NMR spectra were recorded on a Jeol JNM-FX-200 (200/50.1) or a Bruker AV-400 (400/100 MHz) equipped with a pulsed field gradient accessory. Chemical shifts are given in ppm (δ) relative to tetramethylsilane as an internal standard. Coupling constants are given in Hz. All presented ^{13}C-APT spectra are proton decoupled. Optical rotations were measured on a Propol automatic polarimeter (sodium D line, λ = 589 nm), and ATR-IR spectra were recorded on a Shimadzu FTIR-8300 fitted with a single bounce DurasamplIR diamond crystal ATR element. UV spectra were recorded on a Perkin Elmer, Lambda 800 UV/VIS spectrometer. Epoxomicin [17], dansyl-Ahx_3L_3VS [7], NLVS [8], ZLVS [8], ada-Ahx_3L_3VS [6], and Boc-L_3VS [8] were synthesized as described in the literature. Supplemental Data on the synthesis of Bodipy TMR succimidyl ester, **5**, are available.

TFA·L_3VS, 2

Boc-L_3VS (**1**) (0.47 g, 0.9 mmol) was dissolved in a mixture of TFA/DCM (1/1) and was stirred for 30 min. The reaction mixture was concentrated in vacuo and afforded the TFA salt, **2**, as a white solid was used without further purification.

Fmoc-Ahx_3-Wang, 3

Wang resin (1.8 g, 1.1 mmol/g, 2 mmol) was coevaporated with DCE (2×) and was condensed with Fmoc-Ahx-OH (2.1 g, 6 mmol, 3 equiv.) under the influence of DIC (1.0 ml, 6.6 mmol, 3.3 equiv.) and DMAP (12 mg, 0.1 mmol, 0.05 equiv.) for 2 hr. The resin was then filtered and washed with DCM (3×) and subjected to a second condensation sequence. The loading of the resin was determined to be 0.8 mmol/g (2.30 g, 1.84 mmol, 92%) by spectrophotometric analysis. The obtained resin was submitted to two cycles of Fmoc solid-phase synthesis with Fmoc-Ahx-OH, as follows: (i) deprotection with piperidine/NMP (1/4, v/v, 15 min); (ii) wash with NMP (3×); (iii) coupling of Fmoc-Ahx-OH (1.63 g, 4.6 mmol, 2.5 equiv.) in the presence of BOP (2.0 g, 4.6 mmol, 2.5 equiv.) and DiPEA (0.91 ml, 5.5 mmol, 3 equiv.) in NMP and shaken for 2 hr; (iv) wash with NMP (3×) and DCM (3×). Couplings were monitored for completion by the Kaiser test [18].

Fmoc-Ahx_3L_3VS, 4

The tripeptide Fmoc-Ahx_3-OH was released from resin **3** (0.45 mmol) by treatment with TFA/DCM (1/1, v/v, 30 min, 3×). The fractions were collected and coevaporated with toluene (3×). The crude Fmoc-Ahx_3-OH was dissolved in DCM/DMF (99/1, v/v) and condensed with the crude TFA·L_3VS (**2**) (0.9 mmol, 2 equiv.), under the influence of BOP (0.49 g, 1.13 mmol, 2.5 equiv.) and DiPEA (0.45 ml, 2.7 mmol, 6 equiv.). The reaction mixture was stirred overnight, before being concentrated in vacuo. The residue was dissolved in chloroform and washed with 1 M HCl and sat. aq. $NaHCO_3$. The organic layer was dried over $MgSO_4$ and concentrated. Silica column chromatography (DCM → 4% MeOH in DCM) yielded the title compound, **4** (0.41 g, 0.44 mmol, 98%). ^{1}H-NMR (500 MHz, $CDCl_3$/MeOD): δ 7.77 (d, *J* 7.5 Hz, 2H), 7.61 (d, *J* 7.5 Hz, 2H), 7.40 (t, *J* 7.5 Hz, 2H), 7.31 (t, *J* 7.5 Hz, 2H), 6.82 (dd, *J* 15 Hz, *J* 5.0 Hz, 1H), 6.52 (d, *J* 15 Hz, 1H), 4.68 (m, 1H), 4.36 (m, 4H), 4.21 (t, *J* 6.8 Hz, 1H), 3.16 (m, 6H), 2.93 (s, 3H), 2.26–2.14 (m, 6H), 1.62–1.40 (m, 21H), 0.95–0.89 (m, 18H). ^{13}C-NMR (125.8 MHz, $CDCl_3$): δ 174.15, 173.95, 173.87, 173.04, 172.96, 171.98, 171.90, 156.82, 156.78, 147.50, 143.66, 141.00, 128.84, 127.42, 124.74, 124.58, 119.67, 66.25, 51.82, 51.75, 47.62, 47.52, 46.95, 42.35, 42.15, 40.41, 40.28, 39.95, 38.88, 38.75, 35.92, 35.81, 35.49, 29.09, 28.59, 26.02, 25.94, 25.88, 25.06, 24.96, 24.84, 24.54, 24.50, 25.44, 22.52, 22.50, 22.48, 21.46, 21.36. ATR-IR (thin film): 3294.2, 2935.5, 2862.2, 1685.7, 1627.8, 1539.1, 1450.4, 1365.5, 1307.6, 1257.5, 1130.2, 1080.1, 968.2, 833.2, 736.8, 667.3, 621.0 cm^{-1}. HRMS: calculated for $C_{53}H_{82}N_6O_9SH$ 979.59368, found 979.59276.

Bodipy TMR-Ahx_3L_3VS, 6

DBU (30 μl, 0.2 mmol, 1 equiv.) was added to a solution of **4** (0.2 g, 0.2 mmol) in DMF. After 5 min of stirring, HOBt (0.12 g, 0.9 mmol, 4.5 equiv.) was added. To this mixture, Bodipy TMR-OSu (**5**) (0.1 g, 0.2 mmol, 1 equiv.) and DiPEA (0.2 ml, 1.2 mmol, 6 equiv.) were added, and the mixture was stirred for 30 min before being concentrated in vacuo. Purification by column chromatography (0.1% TEA in DCM → 3% MeOH, 0.1% TEA in DCM) afforded Bodipy TMR-Ahx_3L_3VS (**6**) (0.22 g, 197 μmol, 99%). ^{1}H-NMR (500 MHz, $CDCl_3$): δ 7.87 (d, *J* 8.5 Hz, 2H), 7.52 (s, 1H), 7.51 (s, 1H), 7.35 (d, *J* 8 Hz, 1H), 6.97 (m, 5H), 6.81 (dd, *J* 15 Hz, 5 Hz, 1H), 6.79 (s, 1H), 6.55 (d, *J* 4 Hz, 1H), 6.51 (d, *J* 15 Hz), 4.67 (m, 1H), 4.33 (m, 2H), 3.86 (s, 3H), 3.17–3.10 (m, 6H), 2.96 (s, 3H), 2.74 (t, *J* 7.3, 2H), 2.53 (s, 3H), 2.30 (t, *J* 7.3, 2H), 2.21 (m, 5H), 2.14 (t, *J* 7.3, 2H), 2.08 (t, *J* 7.3, 2H), 1.66–1.17 (m, 27H), 0.95–0.89 (m, 18H). ^{13}C-NMR (125.8 MHz, $CDCl_3$): δ 174.40, 174.01, 173.94, 173.20, 172.53, 172.45, 172.06, 160.16, 159.44, 155.16, 147.61, 140.04, 134.77, 134.23, 130.46, 128.87, 128.30, 127.81, 125.29, 122.72, 118.10, 113.55, 55.12, 52.11, 52.04, 47.72, 45.98, 42.46, 42.26, 40.33, 40.00, 39.08, 38.94, 38.80, 35.93, 35.74, 35.62, 28.63, 28.49, 26.04, 25.99, 25.86, 25.03, 24.96, 24.88, 24.63, 24.60, 24.55, 22.66, 22.62, 22.58, 21.54, 21.48, 21.43, 20.09, 12.84, 9.27, 8.36. ATR-IR (thin film): 3290.3, 2927.7, 2866.0, 2160.1, 1975.0, 1631.7, 1604.7, 1539.1, 1461.9, 1434.9, 1369.4, 1292.2, 1230.5, 1203.5, 1172.6, 1130.2, 1056.9, 968.2, 833.2, 779.2, 659.6 cm^{-1}. HRMS: calculated for $C_{59}H_{91}BF_2N_8O_9SH$ 1137.67636, found 1137.67442; for $C_{59}H_{91}BF_2N_8O_9SNH_4$ 1154.70291, found 1154.70149; for $C_{59}H_{91}BF_2N_8O_9SNa$ 1159.65831, found 1159.65690. $[\alpha]_D^{23}$: −44 (c = 0.1, MeOH). λ_{max} (MeOH): 544.43 nm, ε: 60400 liter $mol^{-1}cm^{-1}$.

Bodipy TMR-Ahx_3L_3ES, 7

A catalytic amount of 10% Pd on charcoal was added to a solution of **4** (49 mg, 50 μmol) in MeOH. Hydrogen gas was bubbled through the solution for 2 hr, after which the catalyst was filtered of and the reaction mixture was concentrated in vacuo. The residue was dissolved in DMF and treated with DBU (7.5 μL, 50 μmol, 1 equiv.) for 5 min before HOBt (30 mg, 0.23 mmol, 4.5 equiv.) was added. To this mixture, Bodipy TMR-OSu (**5**) (25 mg, 50 μmol, 1 equiv.) and DiPEA (50 μl, 0.3 mol, 6 equiv.) were added, and the mixture was stirred for 30 min before being concentrated in vacuo. Purification by column chromatography (0.1% TEA in DCM → 3% MeOH, 0.1% TEA in DCM) yielded Bodipy TMR-Ahx_3L_3ES (**7**) (50.3 mg, 44 μmol, 88 %). ^{1}H-NMR (500 MHz, $CDCl_3$/MeOD): δ 7.78 (d, *J* 8.5 Hz, 2H), 7.41 (m, 1H), 7.18 (m, 1H), 7.08 (m, 3H), 6.80 (m, 3H), 6.47 (d, *J* 4 Hz, 1H), 4.18 (m, 2H), 3.92 (m, 1H), 3.78 (s, 3H), 3.07–2.99 (m, 6H), 2.87

(s, 3H), 2.65 (t, *J* 7.5, 2H), 2.44 (s, 3H), 2.22 (t, *J* 7.5, 2H), 2.14 (m, 5H), 2.06 (t, *J* 7.3, 2H), 1.99 (t, *J* 7.5, 2H), 1.95 (m, 1H), 1.77 (m, 1H), 1.56–1.11 (m, 27H), 0.88–0.78 (m, 18H). ^{13}C-NMR (125.8 MHz, $CDCl_3$): δ 174.57, 174.05, 173.14, 172.56, 172.39, 172.31, 160.10, 159.38, 155.08, 140.01, 134.72, 134.18, 130.39, 128.76, 127.96, 127.76, 125.23, 122.70, 117.34, 55.03, 52.26, 52.15, 51.28, 46.03, 45.95, 43.64, 40.17, 40.11, 39.90, 38.91, 38.78, 35.83, 35.77, 35.68, 35.45, 28.56, 28.41, 27.87, 26.02, 25.96, 25.84, 25.02, 24.96, 24.83, 24.63, 24.57, 24.53, 22.72, 22.52, 21.51, 21.37, 21.23. ATR-IR (thin film): 3274.9, 2929.7, 2869.9, 1635.5, 1604.7, 1527.5, 1461.9, 1436.9, 1386.7, 1292.2, 1234.4, 1201.6, 1174.7, 1136.9, 1120.6, 1058.8, 1029.9, 972.1, 839.0, 786.9, 717.5, 663.5 cm^{-1}. HRMS: calculated for $C_{59}H_{93}BF_2N_8O_9SH$ 1139.69201, found 1139.69203.

Proteasomal Activity Measurement with Fluorogenic Substrates

Protein lysates from EL-4 (1 mg/ml) were incubated with various concentrations of MV151 (**6**) for 1 hr at 37°C. For measurement of proteasomal activities, 10 μg labeled lysate was added to 100 μl substrate buffer, containing 20 mM HEPES (pH 8.2), 0.5 mM EDTA, 1% DMSO, 1 mM ATP, and 10 μM Z-Ala-Ala-Arg-AMC (tryptic-like), 60 μM Suc-Leu-Leu-Val-Tyr-AMC (chymotryptic-like), or 60 μM Z-Leu-Leu-Glu-βNA (caspase-like). Fluorescence was measured every minute for 25 min at 37°C by using a Fluostar Optima 96-well plate reader (BMG Labtechnologies) ($\lambda_{ex}/\lambda_{em}$ = 355/450 nm for AMC and 320/405 nm for βNA), and the maximum increase in fluorescence per minute was used to calculate specific activities of each sample. Nonspecific hydrolysis was assessed by preincubation with 1 μM epoxomicin for 1 hr at 37°C and was subtracted from each measurement.

In-Gel Detection of Labeled Proteasome Subunits

Whole-cell lysates were made in lysis buffer containing 50 mM Tris (pH 7.5), 1 mM DTT, 5 mM $MgCl_2$, 250 mM sucrose, 2 mM ATP. Protein concentration was determined by the colorimetric Bradford method. For the labeling reactions, 10 μg total protein lysates was incubated for 1 hr at 37°C with increasing concentrations of MV151 in a total reaction volume of 10 μl. Where indicated, 50 ng purified 20S proteasome (BioMol) was used. For competition studies, cell lysates (10 μg) were exposed to the known inhibitors for 1 hr prior to incubation with MV151 (0.1 μM) for 1 hr at 37°C. For assessment of background labeling, heat-inactivated lysates (10 μg, boiled for 3 min with 1% SDS) were treated with MV151. Reaction mixtures were boiled with Laemmli's buffer containing β-mercapto-ethanol for 3 min and were resolved on 12.5% SDS-PAGE. In-gel visualization was performed in the wet gel slabs directly by using the Cy3/Tamra settings (λ_{ex} 532, λ_{em} 560) on the Typhoon Variable Mode Imager (Amersham Biosciences). Labeling profiles in living cells were determined by incubating ~1 × 10^6 cells with 1–10 μM MV151 in culture medium at 37°C for 8 hr. Cells were lysed, and in-gel detection was carried out as described above.

Cell Culture

The human cervical epithelial carcinoma cell line HeLa, the human melanoma cell line MelJuSo, and the murine lymphoid cell line EL-4 were cultured in RPMI medium (Sigma-Aldrich) supplemented with 10% fetal calf serum (Sigma-Aldrich), 10 U/ml penicillin, and 10 μg/ml streptomycin (Sigma-Aldrich).

Microscopy

Some 0.5 × 10^6 cells were seeded on 35 mm petri dishes with 14 mm microwell nr 1.5 coverslips and on glass-bottomed microwell dishes (MatTek Corp., Ashland, MA) and were allowed to attach overnight. Cells were visualized with a 60× oil immersion lens (Nikon) on a Nikon Eclipse TE 2000U microscope equipped with a Radiance 2100 MP integrated laser and detection system (BioRad) and a Tsunami Multiphoton laser module (Spectra Physics). LaserSharp 2K (BioRad) software was used for microscope control and data acquisition, and Image Pro 3DS 5.1 (Media Cybernetics, Inc.) software was used for image processing. GFP was excited at λ_{ex} = 488 nm and was detected at 500–530 nm. MV151 and MV152 were excited at λ_{ex} = 543 nm and were detected at 560–620 nm. CLSM images were adjusted for brightness and contrast by using Photoshop software.

Mouse Experiments

All animal experiments were approved by the Ethical Committee in Stockholm (ethical permission numbers N-46/04 and N18/05). Mice were housed according to Swedish animal care protocols with a 12 hr day/light cycle, and they were fed standard laboratory chow and tap water ad libitum. Adult C57Bl/6 and Ub^{G76V}-GFP/1 mice [16], matched for sex and age, were given a single intraperitoneal injection of vehicle (60% DMSO, 40% PBS), MV151 (20 μmol/kg body weight), or MG262 (Affiniti) (5 or 10 μmol/kg body weight) in a total volume of 200 μl. Based on prior experience in our lab, the boronic acid inhibitors proved to be more potent and showed better tissue penetration in vivo compared to the vinyl sulfone inhibitors. Therefore, the 20 μmol/kg bodyweight dose was chosen for MV151, which showed no apparent toxicity in mice. Mice were euthanized 24 hr postinjection by anesthetization with inhaled isoflurane (4.4% in oxygen), followed by transcardial perfusion with 50 ml PBS for removal of contaminating blood. Tissues collected for immunocytochemical analysis were processed as described previously [16]. Briefly, 12 μm cryosections were fixed for 15 min in 4% paraformaldehyde/PBS and washed in PBS; where mentioned, Hoechst nuclear stain (2 μg/ml in H_2O) was applied for 15 min in the dark, followed by washing in PBS. Sections were mounted in a matrix containing 2.5% DABCO (Aldrich). Confocal microscopy was performed on a Zeiss LSM 510 META system. Tissues isolated for in-gel analysis were lysed with a Heidolph tissue homogenizer in 300 μl lysis buffer and were further treated as described above.

Supplemental Data

Supplemental Data include information on the synthesis and analytical data of the Bipody TMR-succimidyl ester, **5**, and are available at http://www.chembiol.com/cgi/content/full/13/11/1217/DC1/.

Acknowledgments

The work in the H.S.O. lab was supported by the Netherlands Organization for Scientific Research (NWO) and the Netherlands Proteomics Centre. The work in the N.P.D. lab was supported by the Swedish Research Council, the Swedish Cancer Society, the Nordic Center of Excellence "Neurodegeneration," the Marie Curie Research Training Network (MRTN-CT-2004-512585), and the Karolinska Institutet. Work in the H.O. lab was supported by a grant from the Netherlands Cancer Society (Koningin Wilhelmina Fonds). The authors declare that there are no conflict-of-interest issues.

Received: March 6, 2006
Revised: August 21, 2006
Accepted: September 20, 2006
Published: November 27, 2006

References

1. Rock, K.L., and Goldberg, A.L. (1999). Degradation of cell proteins and the generation of MHC class I-presented peptides. Annu. Rev. Immunol. *17*, 739–779.
2. Baumeister, W., Walz, J., Zuhl, F., and Seemuller, E. (1998). The proteasome: paradigm of a self-compartmentalizing protease. Cell *92*, 367–380.
3. Voges, D., Zwickl, P., and Baumeister, W. (1999). The 26S proteasome: a molecular machine designed for controlled proteolysis. Annu. Rev. Biochem. *68*, 1015–1068.
4. Kisselev, A.F., and Goldberg, A.L. (2001). Proteasome inhibitors: from research tools to drug candidates. Chem. Biol. *8*, 739–758.
5. Ovaa, H., Overkleeft, H.S., Kessler, B.M., and Ploegh, H.L. (2006). Dissecting intracellular proteolysis using small molecule inhibitors and molecular probes. In Protein Degradation: The Ubiquitin System, *Volume 3*, J.R. Mayer, A.J. Ciechanover, and M. Rechsteiner, eds. (Hoboken, NJ: Wiley), pp. 51–78.
6. Kessler, B.M., Tortorella, D., Altun, M., Kisselev, A.F., Fiebiger, E., Hekking, B.G., Ploegh, H.L., and Overkleeft, H.S. (2001). Extended peptide-based inhibitors efficiently target the proteasome and reveal overlapping specificities of the catalytic β-subunits. Chem. Biol. *8*, 913–929.
7. Berkers, C.R., Verdoes, M., Lichtman, E., Fiebiger, E., Kessler, B.M., Anderson, K.C., Ploegh, H.L., Ovaa, H., and Galardy, P.J.

(2005). Activity probe for in vivo profiling of the specificity of proteasome inhibitor bortezomib. Nat. Methods *2*, 357–362.

8. Bogyo, M., McMaster, J.S., Gaczynska, M., Tortorella, D., Goldberg, A.L., and Ploegh, H. (1997). Covalent modification of the active site threonine of proteasomal β subunits and the *Escherichia coli* homolog HslV by a new class of inhibitors. Proc. Natl. Acad. Sci. USA *94*, 6629–6634.
9. Kang, H.C., and Haugland, R.P. December 1993. U.S. patent 5,274,113.
10. Kang, H.C., and Haugland, R.P. September 1995. U.S. patent 5,451,663.
11. Haugland, R.P., and Kang, H.C. September 1988. U.S. patent 4,774,339.
12. Boiadjiev, S.E., and Lightner, D.A. (2003). Syntheses and properties of benzodipyrrinones. J. Heterocycl. Chem. *40*, 181–185.
13. Hideshima, T., Richardson, P., Chauhan, D., Palombella, V.J., Elliott, P.J., Adams, J., and Anderson, K.C. (2001). The proteasome inhibitor PS-341 inhibits growth, induces apoptosis, and overcomes drug resistance in human multiple myeloma cells. Cancer Res. *61*, 3071–3076.
14. Dantuma, N.P., Lindsten, K., Glas, R., Jellne, M., and Masucci, M.G. (2000). Short-lived green fluorescent proteins for quantifying ubiquitin/proteasome-dependent proteolysis in living cells. Nat. Biotechnol. *18*, 538–543.
15. Reits, E.A., Benham, A.M., Plougastel, B., Neefjes, J.J., and Trowsdale, J. (1997). Dynamics of proteasome distribution in living cells. EMBO J. *16*, 6087–6094.
16. Lindsten, K., Menendez-Benito, V., Masucci, M.G., and Dantuma, N.P. (2003). A transgenic mouse model of the ubiquitin/proteasome system. Nat. Biotechnol. *21*, 897–902.
17. Sin, N., Kim, K.B., Elofsson, M., Meng, L., Auth, H., Kwok, B.H., and Crews, C.M. (1999). Total synthesis of the potent proteasome inhibitor epoxomicin: a useful tool for understanding proteasome biology. Bioorg. Med. Chem. Lett. *9*, 2283–2288.
18. Kaiser, E., Colescott, R.L., Bossinger, C.D., and Cook, P.I. (1970). Color test for detection of free terminal amino groups in the solid-phase synthesis of peptides. Anal. Biochem. *34*, 595–598.